Journal of Alloys and Compounds 503 (2010) 159–162

Contents lists available at ScienceDirect

Journal of Alloys and Compounds

journal homepage: www.elsevier.com/locate/jallcom

Preparation of a novel $Bi_{3.64}Mo_{0.36}O_{6.55}$ nanophotocatalyst by molten salt method and evaluation for photocatalytic decomposition of rhodamine B

Lijin Xie[a,*], Zaimei Liu[b], Jianbo Zhang[b], Junfeng Ma[c]

[a] YuYao Environmental Protection Bureau, Zhejiang, Yuyao 315400, China
[b] Ningbo Entry-Exit Inspection and Quarantine Bureau, Zhejiang, Ningbo 315012, China
[c] State Key Laboratory of Green Building Materials, China Building Materials Academy, Beijing 100024, China

ARTICLE INFO

Article history:
Received 11 September 2007
Received in revised form 30 April 2010
Accepted 30 April 2010
Available online 7 May 2010

Keywords:
Photocatalyst
Bismuth molybdate
Nanoparticle
Low temperature molten salt
Rhodamine B

ABSTRACT

Bismuth molybdate ($Bi_{3.64}Mo_{0.36}O_{6.55}$) powders as a novel photocatalyst was prepared using $Bi(NO_3)_3{\cdot}5H_2O$ and $Na_2MoO_4{\cdot}2H_2O$ as raw materials by a simple low temperature molten salt method at 160 °C for 2 h. The as-prepared samples were characterized with X-ray diffraction (XRD), transmission electron microscopy (TEM) and UV–visible (UV–vis) absorption spectra. The photocatalytic activity of $Bi_{3.64}Mo_{0.36}O_{6.55}$(BMO) nanocrystals was evaluated using the photocatalytic oxidation of rhodamine B (RhB) at room temperature under ultraviolet irradiation. The factors affecting the photocatalytic activity, such as photocatalysts concentration, RhB concentration and compressed air as the assisted oxidant species additives, had been studied.

1. Introduction

Photocatalytic degradation of organic compounds using semiconductors has been the subject of extensive studies as a potential way of solving energy and environmental issues over the past two decades [1–7]. Most investigations have focused on anatase-type TiO_2, because it exerts a relatively high photocatalytic activity under irradiation of light with wavelength $\lambda < 390$ nm and high chemical stability [8–10]. In addition, TiO_2 has another advantage of relatively low cost. However, their reactivity and selectivity are not enough for large-scale applications. On the other hand, because of the value of its band gap (3.2 eV), TiO_2 is effective only under ultraviolet irradiation ($\lambda < 390$ nm). Sunlight comprises less than 4% ultraviolet light, so it is a challenge to develop new photocatalysts with high photocatalytic properties to extend the absorbed wavelength range into the visible region, where less expensive light sources exist.

In the past several years, to develop new photocatalysts active under visible light, various efforts have been made so far. Especially, there are a number of studies related to the photocatalytic activity of containing Bi ion compounds, such as Bi_2O_3 [11], Bi_2S_3 [12], $Bi_{12}TiO_{20}$ [13], $Bi_2Ti_2O_7$ [14], Bi_2InNbO_7 [15], Bi_2WO_6 [16], $BiVO_4$ [17] and Bi_2MoO_6 [18]. Their photocatalytic activities are mainly attributed to their crystal structures.

Unfortunately, to the best of our knowledge, $Bi_{3.64}Mo_{0.36}O_{6.55}$(BMO) has not been utilized as photocatalysts. In the present study, we report a simple and effective method for the preparation of nanoscale BMO powders by the low temperature molten salt (LTMS) method. The characterization for as-prepared powders was carried with various methods, including X-ray diffraction (XRD), transmission electron microscopy (TEM) and UV–visible (UV–vis) absorption spectra. Here, we report for the first time the application of BMO for photocatalytic decomposition of RhB under the UV light. RhB ($C_{28}H_{31}N_2O_3Cl$, its structure is presented in Fig. 1) is one of the most important xanthene dyes, which has been well studied [19–21]. The parameters studied include photocatalysts concentration, the pH value of the reaction suspension, RhB concentration and compressed air as the assisted oxidant species additives.

2. Experimental

2.1. Preparation of nanosize BMO

BMO crystals were synthesized by a low temperature molten salt (LTMS) method with analytic reagent grade (99%) chemicals of bismuth nitrate ($Bi(NO_3)_3{\cdot}5H_2O$) and sodium molybdate ($Na_2MoO_4{\cdot}2H_2O$). The whole procedure included the following steps: at first, stoichiometric amounts of $Bi(NO_3)_3{\cdot}5H_2O$ and $Na_2MoO_4{\cdot}2H_2O$ were dissolved into a dilute HNO_3 aqueous solution. After the above mixed solution became clear by constant stirring, it was put into a beaker and then dried in air at 70 °C. When the solvent evaporated completely, the white residue was obtained and used as a precursor. The precursor was mixed with $LiNO_3$–KNO_3 (weight ratio of $LiNO_3/KNO_3 = 2/3$) salt by grinding in a weight ratio of 1:8 of the precursor to the salt. The above mixture was placed in a crucible, and heated at 160 °C for 2 h. The resulting products were thoroughly washed with dilute ammonia water to remove residual

* Corresponding author. Tel.: +86 57462838190; fax: +86 57462838190.
E-mail address: xie_li_jin@yahoo.com.cn (L. Xie).

0925-8388/$ – see front matter © 2010 Elsevier B.V. All rights reserved.
doi:10.1016/j.jallcom.2010.04.221

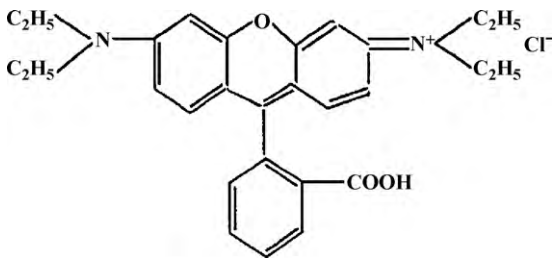

Fig. 1. Chemical structure of rhodamine B.

lithium salt, and washed with distilled water and absolute alcohol for several times, and finally, dried at 80 °C overnight.

2.2. Characterization of as-prepared samples

To determine the crystal phase composition of the prepared powders, X-ray diffraction (XRD) measurement was carried out at room temperature using a Rigaku D/max diffractometer (Japan) with Cu Kα radiation (λ = 1.5406 Å). The accelerating voltage of 40 kV, emission current of 100 mA and the scanning speed of 6°/min were used. A JEM-1200 EX transmission electron microscope (Japan) was employed to examine the particle size and morphology of the as-prepared powders, operated at 60.0 kV. Samples were prepared by adding ethanol to a fraction of the powders synthesized, and droplet of it was dropped on a carbon-coated copper grid. To determine the band gap energy of the photocatalysts, UV–vis absorption spectra were recorded in the wavelength range of 200–1000 nm using a U-3010 spectrophotometer (Japan). Samples for UV–vis characterization were prepared by dispersing the as-prepared powders in the absolute ethanol by ultrasonic, and the absolute ethanol was used as a reference sample.

2.3. Photocatalytic experiments

Photocatalytic experiments were conducted using the photocatalysts to photocatalytically degrade RhB in water solution. The RhB is AR grade, obtained from Shanghai Chemical Reagent Corporation. The photocatalytic system consists of three parts: a sealed black box, a 600 ml Pyrex glass vessel and a 400 W high pressure Hg lamp with a major emission at about 365 nm, which was positioned parallel to the Pyrex glass vessel, as shown in Fig. 2. In all experiments, the reaction temperature was kept at 25 ± 2 °C using a circulating water.

Reaction suspensions were prepared by adding an appropriate amount of photocatalyst powders into a 500 ml of aqueous RhB solutions. The compressed air was bubbled into the reaction solution by air pump to ensure a constant supply of oxygen in air to the reaction volume and complete mixing of solution and BMO photocatalysts during the photoreaction. Prior to irradiation, the suspension was ultrasonically sonicated for 20 min and then magnetically stirred in a dark condition for 60 min to establish an adsorption/desorption equilibrium. The suspensions containing RhB and photocatalyst were then irradiated under the UV light.

At given time intervals, analytical samples were taken from the reaction suspension, centrifuged and filtered through a 0.2 μm Millipore filter to remove the photocatalysts, and the filtrate was then analyzed by UV–vis spectrophotometer.

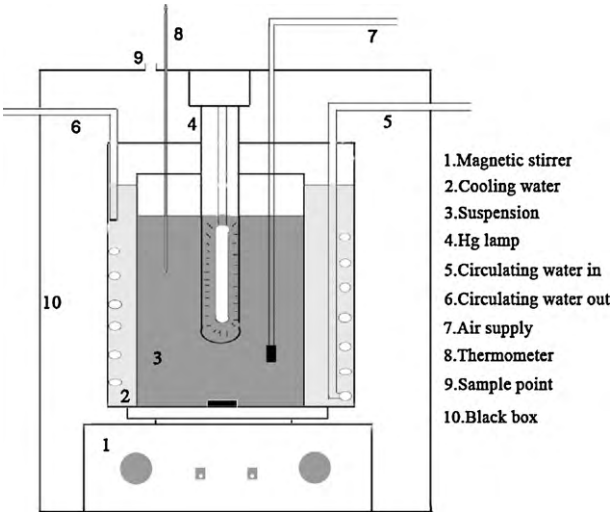

Fig. 2. Schematic diagram of photocatalytic reactor.

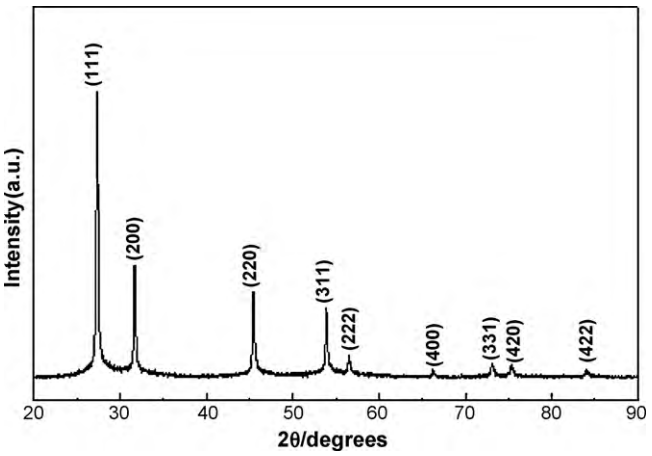

Fig. 3. X-ray diffraction patterns of the $Bi_{3.64}Mo_{0.36}O_{6.55}$ powders synthesized by the LTMS method at 160 °C for 2 h.

3. Results and discussion

3.1. Characterization of the prepared samples

The XRD spectrum of the BMO powders prepared by the LTMS process at 160 °C for 2 h is shown in Fig. 3. All the diffraction peaks in the XRD pattern can be indexed as BMO phase. After refinement, the cell parameters were calculated to be $a = b = c = 5.636$ Å, which were well consistent with the literature data (JCPDS No. 43-0446). No other phases could be detected. The sharp peaks in the XRD patterns indicate a well crystallinity of the prepared samples.

Fig. 4 is the transmission electron microscopy (TEM) micrograph of the BMO powders synthesized by the LTMS method at 160 °C for 2 h. It showed that BMO powders were composed of nano-sized particles, which were about 70 nm in size, and that each particle was nearly spherical in shape and thickness. It could be concluded that nano-sized photocatalyst BMO powders were easily synthesized by our method.

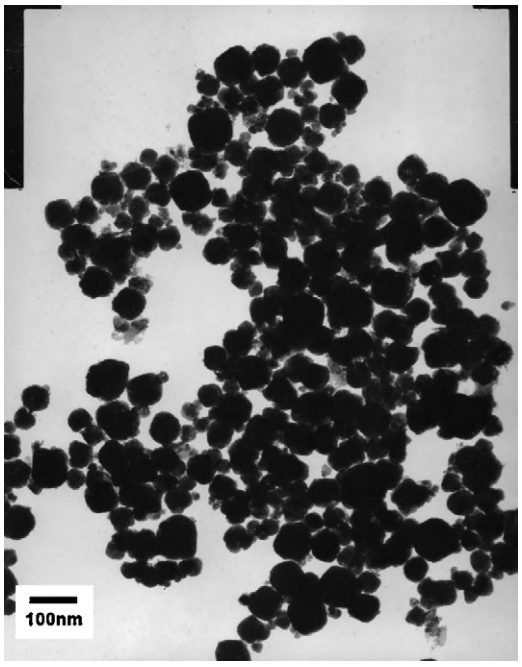

Fig. 4. TEM images of the $Bi_{3.64}Mo_{0.36}O_{6.55}$ powders synthesized by the LTMS method at 160 °C for 2 h.

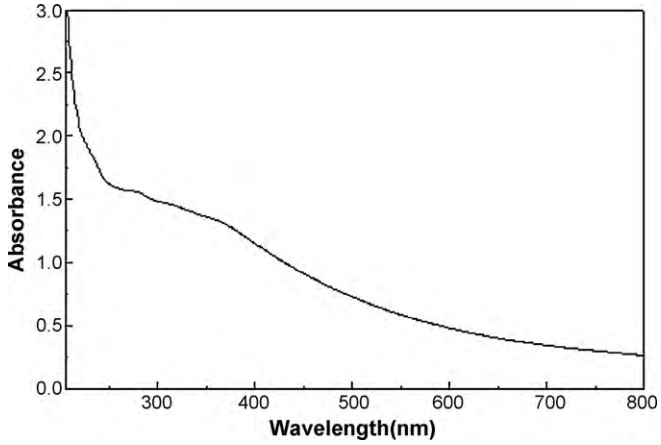

Fig. 5. UV–vis absorption spectrum of the BMO powders prepared by the LTMS method at 350 °C for 2 h.

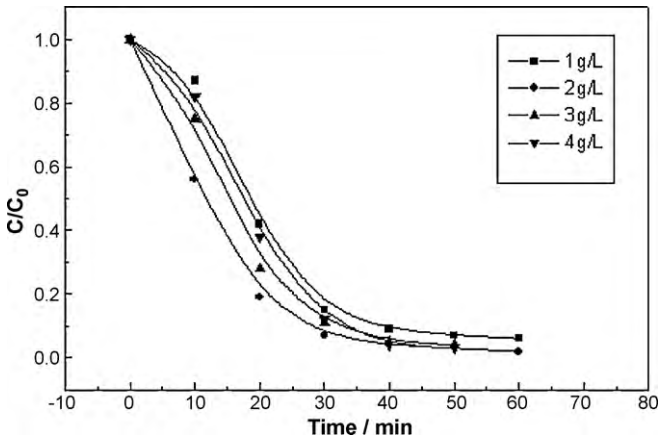

Fig. 6. The effect of the concentration of BMO catalysts on the degradation of RhB under the irradiation of UV light: [RhB] = 20 mg/L; pH = 3.0; with compressed air.

The UV–vis absorption properties of the BMO nanocrystals synthesized by the LTMS method at 160 °C for 2 h are displayed in Fig. 5. As shown in Fig. 4, the band gap adsorption edge of BMO is estimated to be 532 nm corresponding to the band gap energy to be 2.33 eV ($E_g = hc/\lambda$, where h is elementary quantum, c is speed of light, and λ is absorption wave length). It can be expected that the BMO nanocrystals prepared in the present study should have a good photocatalytic potential not only in the ultraviolet light but also in the visible light region.

3.2. Photocatalytic activity of the prepared samples

The band at 554 nm was used to monitor the effect of the photocatalysis on the degradation of RhB because the band was absorption maximum in the UV–vis spectra for RhB solution. It is known that RhB can be adsorbed onto catalysts from its aqueous solution. Hachem et al. [22] pointed out that the absorption was quite fast and the equilibrium concentration could be reached within 45 min. In this paper, the absorption/desorption equilibrium of the suspensions was established by ultrasonically sonicated for 20 min and then magnetically stirred in a dark condition for 60 min. In general, the photocatalytic degradation follows a Langmuir–Hinshelwood mechanism [23,24], with the rate r being proportional to the coverage θ which becomes proportional to C at low concentrations

$$r = k\theta = \frac{k\mathrm{KC}}{1 + \mathrm{KC}} \quad (1)$$

where k is the true rate constant which includes various parameters such as the mass of catalyst, the flux of efficient photons, the coverage in oxygen, etc., and K is the adsorption constant. Since the initial concentration is low ($C_0 = 20$ mg/L), the term KC in the denominator can be neglected and the rate becomes, apparently, first order

$$r = -\frac{\mathrm{d}C}{\mathrm{d}t} = k\mathrm{KC} = k_{\mathrm{app}}C \quad (2)$$

where k_{app} is the apparent rate constant of pseudo-first order. Therefore, the integral form $C = f(t)$ of the rate equation is

$$\ln\frac{C_0}{C} = k_{\mathrm{app}}t \quad (3)$$

3.2.1. Effect of photocatalyst concentration on the photocatalytic activity

In order to determine the optimal amount of photocatalyst, a preliminary study (Fig. 6) has been carried out to optimize the quantity of BMO catalysts, where the amount of the photocatalyst was varied from 1 to 4 g/L. It could be considered that the concentration of RhB decreased negligibly over the time span of these experiments in the absence of photocatalysts. A blank experiment in the absence of irradiation but with the prepared catalysts demonstrated that no significant change in the quantity was found. As shown in Fig. 6, the quantity of BMO catalysts, indeed, has a great effect upon its ability to degrade the aqueous RhB in the photocatalyst quantity range varied from 1 to 4 g/L. The calculated apparent reaction rate constants of each case are listed in Table 1. The experiment results reveal that the degree of degradation of RhB solution increases with increasing the amount of the photocatalyst, and reaches the higher value at catalyst loading = 2 g/L and then decreases. This phenomenon results from the so-called shielding effect; after exceeding the optimal amount, the suspended catalysts reduce the penetration of the light in the solution [25]. Similar phenomena were also found in the study of the TiO_2 and $Bi_2Ti_2O_7$ photocatalysts [14,25], the catalysts quantity were all shown having an optimal amount, to support the catalysts showing the highest activity. Because the most active was the photocatalyst with quantity of 2 g/L, the rest of experiments were carried out using this quantity.

3.2.2. Effect of RhB concentration on the photocatalytic activity

The effect of initial RhB concentration in water on the photocatalytic process was examined. The reactions of RhB decomposition were carried out in the range 20–50 mg/L. As shown in Fig. 7 and Table 2, the degradation efficiency is decreased with the increasing concentrations of RhB. It was found that the best degradation was obtained with 20 mg/L RhB. The result is same with that obtained for the degradation of methyl orange using TiO_2 [26], which can be related to the formation of several layers of adsorbed dye on the photocatalyst surface and then inhibits the reaction of dye molecules with photogenerated holes or hydroxyl radicals. Similar result was also found in the study of the Ti–Ag–US and $Bi_4Ti_3O_{12}$ photocatalysts [27,28].

Table 1
The apparent reaction rate constants calculated from Fig. 6 for various concentrations of $Bi_{3.64}Mo_{0.36}O_{6.55}$ catalyst in RhB solution.

Catalyst concentration	Apparent reaction rate constants k ($\times 10^{-3}$ min^{-1})	RhB degradation (min)[a]
1	56.3	18.6
2	80.9	11.9
3	62.9	15.2
4	47.7	17.4

[a] Time required for 50% degradation of 20 mg/L RhB solution.

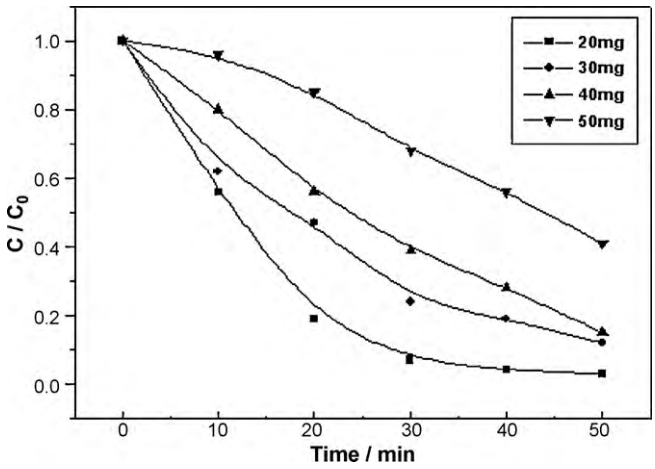

Fig. 7. The effect of initial RhB concentration on the photocatalytic activity of $Bi_{3.64}Mo_{0.36}O_{6.55}$: pH = 3.0; with compressed air.

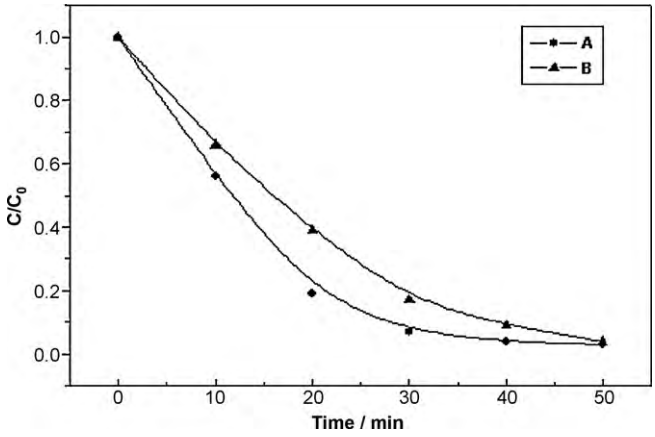

Fig. 8. The effect of compressed air on the degradation of RhB under the irradiation of UV light, A: with compressed air; B: without compressed air; [RhB] = 20 mg/L; pH = 3.0.

3.2.3. *Effect of compressed air on the photocatalytic activity*

In our experiment, the influence of compressed air as the assisted oxidant species additives on the photocatalytic activity of BMO catalysts was also studied. Fig. 8 shows the comparisons of changes of RhB degradation under the irradiation of UV light with compressed air or not. The rate constant values of RhB degradation obtained from Fig. 8 are reported and listed in Table 3. As shown in Fig. 8 and Table 3, the rate constant with compressed air is obviously higher than that without that. The improved catalytic activity of BMO in the presence of compressed air can be attributed to the dissolved oxygen from the compressed air, which can enhance the separation of photogenerated electrons and holes, and then improve the efficiency of producing •OH radical [29]. In addition, the compressed air enables the reaction solution to mix completely, which favor the degradation of RhB.

Table 2
The influence of rhodamine B concentrations on the activity of $Bi_{3.64}Mo_{0.36}O_{6.55}$.

Concentration of rhodamine B (mg/L)	Apparent reaction rate constants k ($\times 10^{-3}$ min^{-1})	Rhodamine B degradation (min)[a]
20	80.9	11.9
30	37.7	17.5
40	29.2	23.8
50	8.1	44.1

[a] Time required for 50% degradation of 20 mg/L RhB solution.

Table 3
The influence of compressed air on the photocatalytic activity of Bi_2MoO_6 catalysts.

Compressed air	Apparent reaction rate constants k ($\times 10^{-3}$ min^{-1})	RhB degradation (min)[a]
With	80.9	11.9
Without	46.9	16.2

[a] Time required for 50% degradation of 20 mg/L RhB solution.

In this paper, the high activity of BMO as a new photocatalyst might be mainly ascribed to the presence of the ion defects in the BMO crystal structure, which can enhance the separation of photogenerated electrons and holes, resulting in the improvement of photocatalytic activities [30,31]. The photocatalytic mechanistic study for RhB degradation is in progress at present.

4. Conclusion

The spherical nanoscale BMO powders as a novel photocatalyst can be successfully synthesized using a simple low temperature molten salt method for the first time. The BMO powders exhibit good photocatalytic properties to photodegrade RhB at room temperature. The photocatalyst concentrations, the RhB concentrations and the compressed air as the assisted oxidant species additives are important factors affecting the photocatalytic activity. Under the irradiation of the high pressure Hg lamp, the high activity of BMO as a new photocatalyst might be mainly ascribed to ion defects, which can enhance the separation of photogenerated electrons and holes. Further work is under way to study the specific mechanism of photocatalytic degradation of RhB on BMO.

References

[1] H. Al-Ekabi, N. Serpone, J. Phys. Chem. 92 (1994) 3315.
[2] S. Kutsuna, Y. Ebihara, K. Nakamura, T. Ibusuki, Atmos. Environ. 27A (1993) 599.
[3] V. Augugliaro, L. Palmisano, M. Scheavello, A. Scalfani, Appl. Catal. A 69 (1991) 323.
[4] O. Legrini, E. Oliveros, A.M. Braum, Chem. Rev. 93 (1993) 671.
[5] M. Anpo, H. Yamashita, Y. Ichihachi, S. Ehara, J. Electroanal. Chem. 396 (1995) 21.
[6] D.F. Ollis, C.Y. Hsiao, L. Budiman, C.L. Lee, J. Catal. 88 (1984) 89.
[7] R.W. Mathews, Sol. Energy 38 (1987) 405.
[8] M.R. Hoffmann, S.T. Martin, W. Choi, D.W. Bahnemann, Chem. Rev. 95 (1995) 69.
[9] K. Honda, A. Fuhishima, Nature 238 (1972) 37.
[10] A. Fujishima, T.N. Rao, D.A. Tryk, J. Photochem. Photobiol. C: Photochem. Rev. 1 (2000) 1.
[11] K. Gurunathan, Int. J. Hydrogen Energy 29 (2004) 933.
[12] Y. Bessekhouad, M. Mohammedi, M. Trari, Sol. Energy Mater. Sol. Cells 73 (2002) 339.
[13] W.F. Yao, H. Wang, X.H. Xu, X.F. Cheng, J. Huang, et al., Appl. Catal. A: Gen. 243 (2003) 185.
[14] W.F. Yao, H. Wang, X.H. Xu, J.T. Zhou, X.N. Yang, et al., Appl. Catal. A: Gen. 259 (2004) 29.
[15] Z.G. Zou, J.H. Ye, H. Arakawa, J. Mol. Catal. A 168 (2001) 289.
[16] J.G. Yu, J.F. Xiong, B. Cheng, Y. Yu, J.B. Wang, J. Solid State Chem. 178 (2005) 1968.
[17] S. Kohtani, M. Koshiko, A. Kudo, K. Tokumura, et al., Appl. Catal. B: Environ. 46 (2003) 573.
[18] A. Martínez-de la Cruz, S. Obregón Alfaro, E. López Cuéllar, U. Ortiz Méndez, Catalysis Today 129 (2007) 194.
[19] Y. Ma, J.N. Yao, Chemosphere 38 (1999) 2407.
[20] Y. Ma, J.N. Yao, J. Photochem. Photobiol. A: Chem. 116 (1998) 167.
[21] T.X. Wu, G.M. Liu, J.C. Zhao, H. Hidaka, N. Serpone, J. Phys. Chem. B 102 (1998) 5845.
[22] C. Hachem, F. Bocquillon, O. Zahraa, M. Bouchy, Dyes Pigments 49 (2001) 117.
[23] A. Houas, H. Lachheb, M. Ksibi, E. Elaloui, C. Guillard, J.-M. Hertmann, Appl. Catal. B: Environ. 31 (2001) 134.
[24] J.C. Yu, J. Yu, J. Zhao, Appl. Catal. B: Environ. 36 (2002) 31.
[25] J. Grzechulska, A.W. Morawski, Appl. Catal. B: Environ. 36 (2002) 45.
[26] A.Q. Siham, R.S. Salman, J. Photochem. Photobiol. A: Chem. 148 (2002) 161.
[27] S. Senthilkumaar, K. Porkodi, R. Gomathi, A. Geetha Maheswari, N. Manonmani, Dyes Pigments 69 (2006) 22.
[28] W.F. Yao, X.H. Xu, F H.W., J.T. Zhou, et al., Appl. Catal. B: Environ. 52 (2004) 109.
[29] W. Nam, J. Kim, G. Han, Chemosphere 47 (2002) 1019.
[30] T. Ishii, H. Kato, A. Kudo, J. Photochem. Photobiol. A: Chem. 163 (2004) 181.
[31] J.J. Liu, Y.C. Yu, H.L. He, X.G. Jin, K. Xu, Mater. Res. Bull. 35 (2000) 377.